American Journal of Environmental Science and Engineering
2026, Vol. 10, No. 3, pp. 74–81
https://doi.org/10.11648/j.ajese.20261003.11

SciencePG
Science Publishing Group

Research Article

Cationic Quaternized Cellulose Separator Enables Selective Polyiodide Regulation for Stable Lithium-Iodine Batteries

Changyong Song, Xuejin Li, Wei Xing*

School of Materials Science and Engineering, State Key Laboratory of Heavy Oil Processing, China University of Petroleum (East China), Qingdao, P. R. China

Abstract

The growing demand of safe and high-energy-density energy storage has spurred renewed interest in rechargeable lithium-iodine (Li-I_2) batteries, which are attractive due to their high theoretical capacity (211 mAh g^{-1} based on iodine) and fast iodine redox reaction kinetics that enable high power output. However, the severe shuttle effect caused by soluble polyiodide intermediates significantly limits the electrochemical reversibility and cycling stability of these batteries. Herein, a cationic quaternized cellulose separator (QCP) is developed to regulate polyiodide transport and interfacial conversion behavior in Li-I_2 batteries. Owing to the introduced quaternary ammonium functional groups, the QCP separator exhibits strong electrostatic interactions with negatively charged polyiodide species, effectively inhibiting their diffusion and stabilizing the iodine redox chemistry. Compared with pristine glass fiber (GF) and cellulose separators (CP), the QCP separator demonstrates higher ionic conductivity, increased lithium-ion transference number, reduced interfacial resistance, and improved electrochemical stability. Consequently, Li-I_2 batteries assembled with the QCP separator show significantly enhanced cycling stability, superior rate capability, and improved reaction kinetics. Moreover, the QCP separator enables more stable lithium deposition/stripping behavior and enhances interfacial compatibility with the lithium metal anode. This work demonstrates an effective strategy for constructing selective ion-regulating interfaces through cationic cellulose engineering and provides new insights for separator design in advanced halogen-based energy storage systems.

Keywords

Lithium-ion Batteries, Quaternized Cellulose Separator, Electrostatic Confinement

1. Introduction

Rechargeable lithium-iodine (Li-I_2) batteries have attracted much attention due to their high theoretical capacity, inherent safety, and rapid redox reaction kinetics derived from the reversible transformation of iodine species [1, 2]. They are regarded as a highly promising electrochemical energy storage system. Particularly, the multi-electron redox chemical properties of iodine endow Li-I_2 batteries with high energy density and excellent rate performance, making them an ideal choice for next-generation portable and large-scale energy storage applications [3, 4]. However, the actual development of Li-I_2

*Correspondence: Wei Xing (xingwei@upc.edu.cn)

Received: 2 June 2026; **Accepted:** 25 June 2026; **Published:** 6 August 2026

batteries has been severely hindered by the complex evolution and migration behavior of soluble polyiodide intermediates during the cycling process [5, 6].

Among various iodine compounds, the triiodide ion (I_3^-) plays a crucial role in determining the electrochemical reversibility and reaction kinetics of lithium-iodine batteries. However, the high solubility and rapid diffusion of polyiodide ions in ether-based electrolytes inevitably lead to severe shuttle effects, resulting in the loss of active materials, slow redox reactions, parasitic reactions on the lithium anode, and rapid capacity degradation [7, 8]. Moreover, the uncontrolled migration of polyiodide ion anions leads to uneven distribution of interface reactions and deterioration of charge transfer kinetics, thereby seriously damaging the long-term cycling stability of lithium-iodine batteries. Therefore, effectively regulating the transport and interface transformation behavior of polyiodide ions is crucial for constructing high-performance lithium-iodine battery systems.

To address these challenges, considerable efforts have been made to design iodine carriers [9, 10], catalytic materials [11], and functional separators (e.g.,[12]) to inhibit the shuttle phenomenon of multiple iodide ions. Polar materials such as metal oxides [13], carbon doped with heteroatoms [14], covalent organic frameworks [15], and polymer materials [16] have been extensively studied. They fix the multiple iodide ions through chemical adsorption or catalytic conversion. Although these strategies can partially alleviate the shuttle effect, excessive adsorption often sacrifices the reversibility of redox and slows down the iodine conversion rate. Moreover, traditional separator modification strategies mainly rely on passive physical barriers or non-specific polar interactions, which are still insufficiently effective for selectively regulating the migration of negatively charged multiple iodide ions.

Compared with traditional glass fiber (GF) membranes, membranes based on cellulose have recently emerged as promising alternatives due to their abundant polar functional groups, excellent electrolyte wettability, porous fiber structure, and good ionic conductivity. The cellulose framework is rich in hydroxyl groups, enhancing the affinity of the electrolyte and promoting the transport of lithium ions, thereby facilitating the interfacial ion transfer in rechargeable batteries. However, the interaction between the original cellulose and polyiodide ions is still mainly dominated by relatively weak polar adsorption, which cannot fundamentally control the diffusion and transformation behavior of polyiodide anions.

Inspired by the electrostatic interaction between cationic functional groups and negatively charged polyiodides, introducing positively charged interfaces into cellulose membranes may provide an effective strategy for selective regulation of polyiodides. Quaternary ammonium groups have a strong electrostatic attraction to polyiodide anions and may restrict polyiodides to local interface regions, thereby inhibiting the shuttle effect and optimizing the iodine conversion pathway. More importantly, the combination of cationic interfaces with ionic conductive cellulose frameworks can simultaneously achieve selective limitation of polyiodides and efficient lithium-ion transmission, which is extremely ideal for improving the electrochemical reversibility and reaction kinetics of lithium iodide batteries.

Here, we report a quaternized cellulose separator (QCP), which is used to regulate the iodide ion transport and interface transformation chemical reactions in lithium-iodine batteries. Compared with the original glass fiber and cellulose separator (CP), QCP introduces cationic quaternary ammonium groups onto the cellulose framework, thereby enhancing the electrostatic interaction with iodide ions. The ion-conductive cellulose network and the synergistic effect of the cationic interface chemistry effectively inhibit the diffusion of iodide ions while maintaining rapid lithium ion transport and low interface resistance. Therefore, the lithium-iodine battery using QCP separator exhibits significant improvement in reaction kinetics, enhanced rate capability, and prolonged cycle stability. This work demonstrates an effective strategy for constructing a selective ion-regulating interface and provides new insights into the separator interface engineering of advanced halogen-based energy storage systems.

2. Experimental Section

2.1. Materials

All chemicals were of analytical grade and used as received without further purification. Iodine (I_2, 99.8%), sodium hydroxide (NaOH, ≥97%), 2,3-Dihydroxy-N,N,N-trimethylpropan-1-aminium (EPTAC, 99%) were bought from Shanghai McLean Biochemical Technology Co., Ltd. Cellulose pulp were bought from Sigma-Aldrich.

2 2. Preparation of Quaternized Cellulose (QCP)

Cationic cellulose nanofibers were synthesized according to a modified literature procedure [17]. Briefly, cellulose pulp (60 g, 25 wt%) was dispersed in deionized water, followed by the addition of EPTAC (7.5 g) and NaOH (2.25 g) to form a homogeneous reaction mixture. The suspension was then diluted with 180 g of isopropanol and stirred at 50 °C for 3 h. Unreacted reagents and by-products were removed by centrifugation, and the resulting product was extensively dialyzed against distilled water using a 14,000 Da molecular weight cutoff membrane for 72 h.

2.3. Materials Characterizations

The chemical structures of the separators were characterized by Fourier transform infrared spectroscopy (FTIR) in the wavenumber range of 4000-500 cm^{-1}. The crystallographic structures of the samples were investigated using X-ray diffraction (XRD) with Cu Kα radiation (λ=1.5406 Å) over a

scanning range of 10-80°. Thermogravimetric analysis (TGA-) was conducted from room temperature to 800 °C under a nitrogen atmosphere at a heating rate of 10 °C min-1 to evaluate the thermal stability of the separators. The surface charge characteristics of the samples were analyzed by zeta potential measurements using a Zeta instrument. The morphologies and microstructures of the separators before and after modification were observed by field-emission scanning electron microscopy (FESEM).

The ionic conductivity of the separators soaked with electrolyte was determined using electrochemical impedance spectroscopy (EIS) based on stainless steel/separator/stainless steel (SS/separator/SS) symmetric cells in the frequency range from 1×10^{-2} to 1×10^{-6} Hz. The ionic conductivity (σ) was calculated according to the following equation:

$$\sigma=\frac{L}{R\times S} \quad (1)$$

where L is the separator thickness, R is the bulk resistance obtained from the Nyquist plot, and S is the electrode area.

The lithium-ion transference number (tLi^+) was evaluated using the combination of AC impedance and DC polarization measurements in Li/separator/Li symmetric cells at a constant polarization voltage of 10 mV. The lithium-ion transference number was calculated according to the Bruce–Vincent–Evans equation:

$$t_{Li^+}=\frac{I_s(\Delta V-I_0R_0)}{I_0(\Delta V-I_SR_S)} \quad (2)$$

where ΔV is the applied polarization voltage, I0 and Is represent the initial and steady-state currents, respectively, and R0 and Rs correspond to the interfacial resistances before and after polarization.

The electrochemical performance of lithium-iodine batteries was evaluated using CR2032-type coin cells was evaluated using CR2032 cylindrical batteries packed in a glove box filled with argon gas. Within the voltage range of 2.0-4.0 V, cyclic voltammetry (CV) measurements were conducted at different scan rates on an electrochemical workstation (CHI 660). At room temperature, constant current charge-discharge measurements were performed using the LAND battery testing system, including cycle and rate performance tests.

To evaluate the interface stability of the separator towards lithium metal, we assembled a lithium/lithium symmetric battery and conducted tests under the same current density. At the same time, the lithium deposition/deposition conditions were repeated. Additionally, an asymmetric lithium/copper battery was assembled to study the reversibility and interface compatibility of lithium deposition/deposition under different separators.

3. Results and Discussion

In order to enhance the polyiodide regulation capability of the cellulose separator, quaternary ammonium groups were introduced onto the cellulose framework through the quaternization process, aiming to construct a cationic interface to achieve selective limitation of polyiodides while maintaining the effective transmission of lithium ions. Firstly, the quaternization process of the cellulose separator was verified by Fourier transform infrared spectroscopy. As shown in Figure 1a, the original CP exhibited characteristic absorption peaks corresponding to the hydroxyl stretching vibration and the C–O–C structure of cellulose. After quaternization treatment, new characteristic peaks related to C–N stretching vibration and quaternary ammonium functional groups appeared in the QCP spectrum, which confirmed the successful introduction of cationic functional groups onto the cellulose framework. These results indicate that the quaternization treatment effectively changed the surface chemical properties of the cellulose separator.

The crystal structures of CP and QCP were further studied by XRD analysis (Figure 1b). The CP exhibited typical cellulose diffraction peaks, indicating that it has an inherent crystal structure. After quaternization treatment, the characteristic diffraction peaks of cellulose remained largely unchanged, suggesting that the modification process did not damage the original fibrous structure of cellulose. The thermal stability of the membrane was evaluated by thermogravimetric analysis. As shown in Figure 1c, compared with the original CP, QCP exhibited obvious thermal decomposition characteristics, which can be attributed to the introduction of quaternary ammonium groups on the cellulose framework.

The surface charge characteristics of the membrane were further characterized by measuring the zeta potential (Figure 1d). Compared with the negatively charged CP membrane, the QCP membrane after quaternization treatment showed a significantly increased positive surface potential, indicating that a cationic interface was successfully constructed. This positively charged surface will have a strong electrostatic interaction with the negatively charged iodide ions, thereby inhibiting their disordered diffusion in the electrolyte.

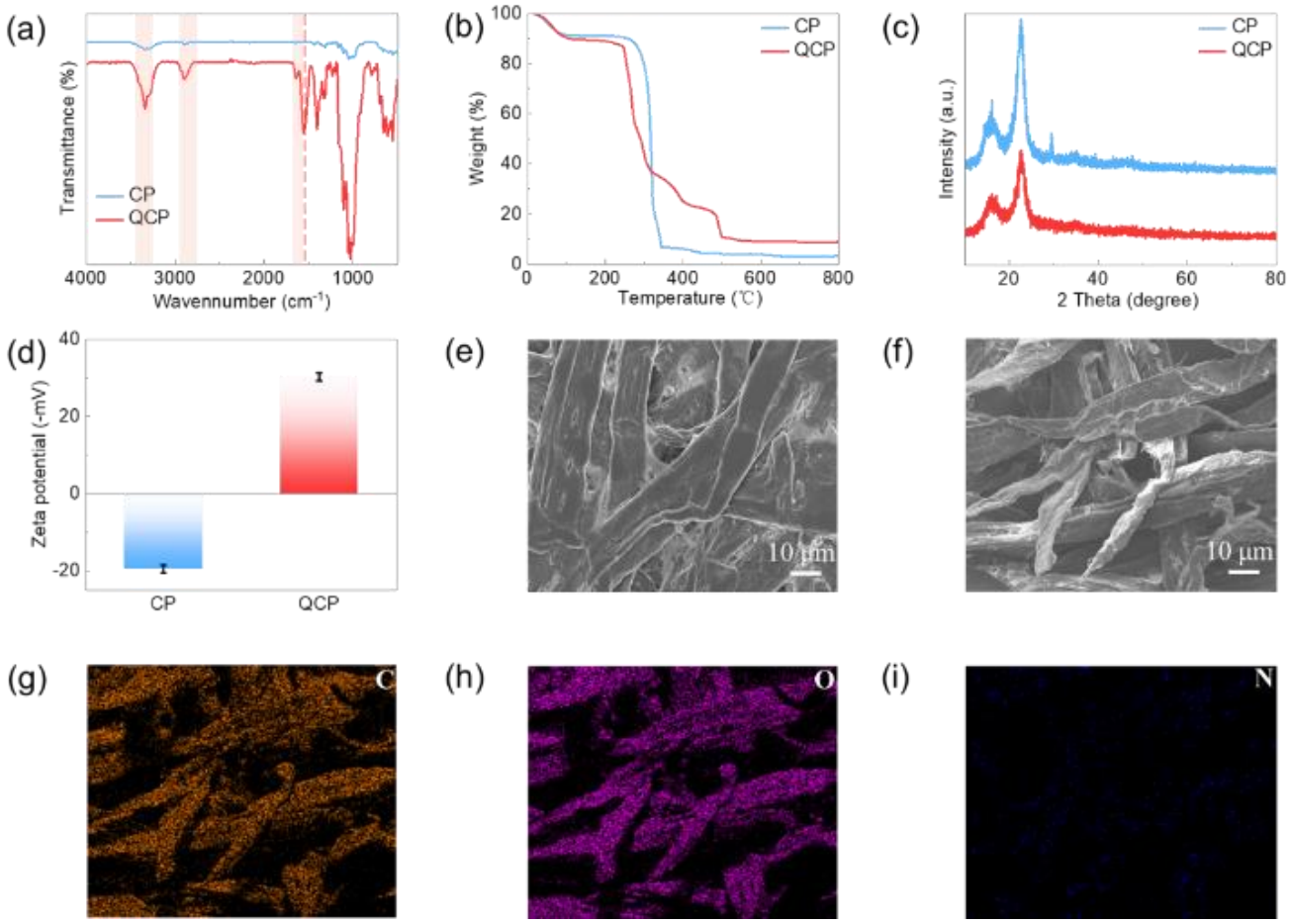

Figure 1. *(a) FT-IR spectra (b) TGA profiles (c) XRD spectra (d) Zeta potential of CP and QCP; SEM image of (e) CP and (f) QCP; The elemental mapping of (g) C, (h) O, and (i) N of QCP.*

The morphology and microstructure of the separator were characterized by scanning electron microscopy. As shown in Figures 1e-g, both CP and QCP maintain a connected fibrous porous structure, which is conducive to the penetration of electrolyte and ion transport. Compared with CP, the surface of the QCP separator after quaternization treatment presents a rough morphology, indicating the success of surface functionalization. Additionally, the elemental distribution images show that nitrogen elements are uniformly distributed throughout the QCP structure, further confirming the uniform introduction of quaternary groups into the cellulose network (Figures 1 g-i). The retained porous structure combined with the uniformly distributed cationic functional groups is expected to simultaneously promote lithium ion transport and regulate the migration behavior of polyiodide ions.

To investigate the adsorption capabilities of different separators towards polyiodide ions, a visual adsorption experiment was conducted using GF, CP, and QCP separators in an electrolyte containing polyiodide ions. As shown in Figure 2, the electrolyte using the GF separator became significantly darker on the right side after 1 h, indicating that it had almost no blocking effect on the dissolved polyiodide ions. In contrast, the QCP separator, due to the interaction between the hydroxyl and quaternary ammonium functional groups and the polyiodide ions, did not show a significant deepening of the solution on the right side after 3 h, indicating that it had a significantly enhanced adsorption ability towards polyiodide ions.

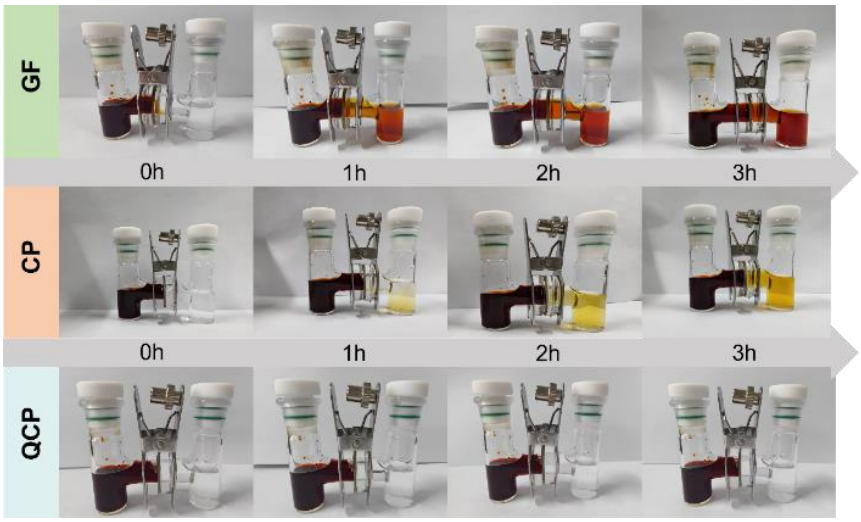

Figure 2. *Time-lapse visualization of polyiodide shuttling in H-type cells equipped with GF, CP, and QCP separators.*

QCP exhibits excellent adsorption performance, which is attributed to the strong electrostatic interaction between the quaternary ammonium groups and the negatively charged polyiodide anions. Unlike the weaker physical adsorption or non-specific polar interactions found in traditional separators, the cation interface in QCP can selectively regulate the diffusion and interface distribution of polyiodide ions through electrostatic constraints. This selective regulation of polyiodide ions is highly beneficial for suppressing shuttle effects, reducing active material loss, and stabilizing the iodine redox chemical reaction during the cycling process.

Efficient lithium-ion transport is crucial for achieving stable electrochemical performance of lithium-iodine batteries. Therefore, a systematic study was conducted on the ionic conductivity, lithium-ion transfer number, electrochemical window, and interface resistance of different separators.

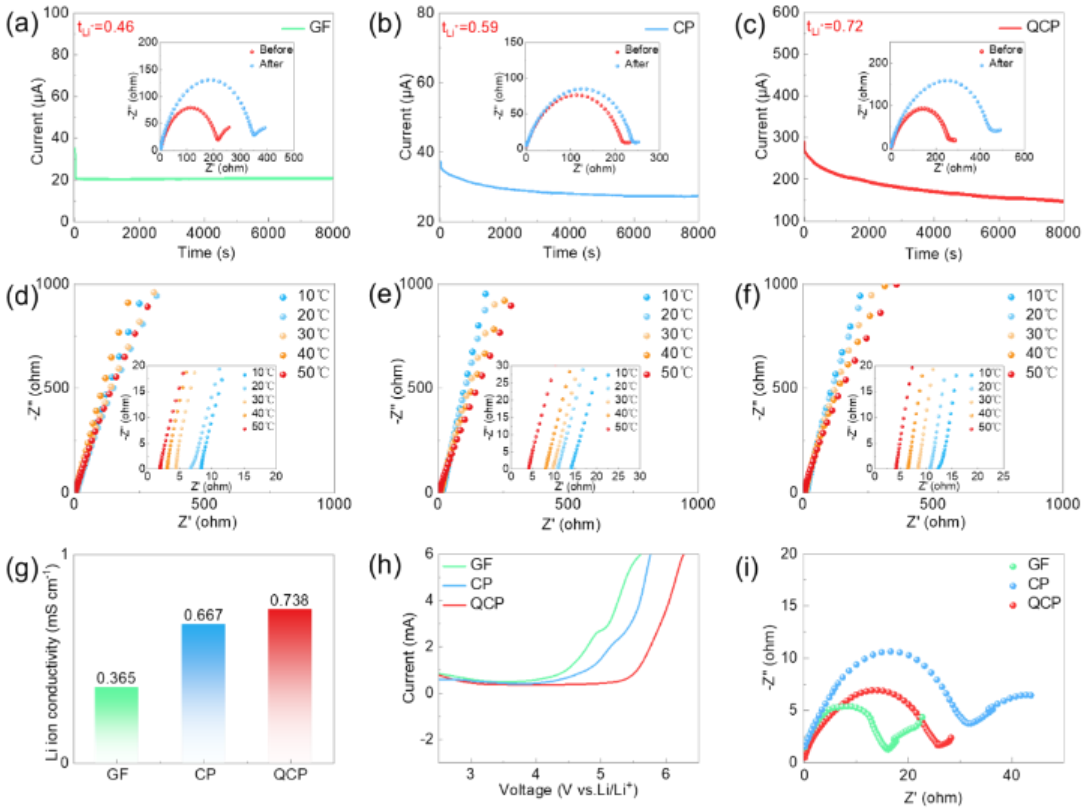

Figure 3. *Current-time curves of (a) GF, (b) CP, and (c) QCP separators-based symmetric Li cells at a polarization voltage of 10 mV. Insets show the corresponding Nyquist plots before and after polarization to measure the Li^+ transference number; EIS plots of (d) GF, (e) CP, and (f) QCP from 10 to 50 ℃; (g) Li^+ conductivity of GF, CP, QCP at 30 ℃; (h) LSV curves of Li||SS cells with GF, CP, QCP; (i) Nyquist plots.*

As shown in Figures 3a-c, the lithium-ion transference number of the QCP separator is higher than those of the GF and CP separators, indicating a stronger selective lithium-ion transport capability. The ionic conductivity results shown in Figures 3d-f further demonstrate that the QCP separator maintains excellent ionic conductivity after quaternization treatment. At 30 °C, its ionic conductivity reaches 0.738 mS cm^{-1}, which is significantly higher than that of the GF separator (Figure 3g). The electrochemical stability of the separators was evaluated by linear sweep voltammetry (LSV). As shown in Figure 3h, the QCP separator exhibits a wider electrochemical window, indicating that the introduced quaternary ammonium groups do not compromise the electrochemical stability of the separator. Further electrochemical impedance spectroscopy (EIS) measurements were conducted to investigate the interfacial charge-transfer behavior. As shown in Figure 3i, the interfacial resistance of the QCP separator is significantly lower than that of the CP separator. This reduction in impedance can be attributed to enhanced electrolyte affinity, efficient lithium-ion transport, and the synergistic effect of regulated polyiodide distribution at the electrode/electrolyte interface.

The electrochemical performance of lithium-iodine batteries assembled with different separators was systematically evaluated. As shown in Figure 4a, the battery assembled with the QCP separator exhibited significantly better cycling stability at 1 C compared to the GF and CP ones. This enhanced cycling performance can be attributed to the effective inhibition of the polyiodide ion shuttle effect, as well as the stable interfacial redox chemical reactions achieved by the cationic separator interface. Rate capability tests further demonstrated the superior kinetic performance of the QCP-based battery (Figure 4b). Even at a high current density of 10 C, the battery assembled with QCP separator showed a higher reversible capacity. The redox kinetics of iodine was studied by cyclic voltammetry. As shown in Figures 4c-e, the battery based on QCP exhibited a smaller peak separation, which indicates an enhanced electrochemical reversibility compared to the GF and CP separators. In addition, an asymmetric lithium/copper battery was assembled to study the reversibility of lithium deposition/peeling. As shown in Figure 4f, the cycling performance of the QCP separator is more stable, indicating that it can suppress side reactions and stabilize the lithium metal interface.

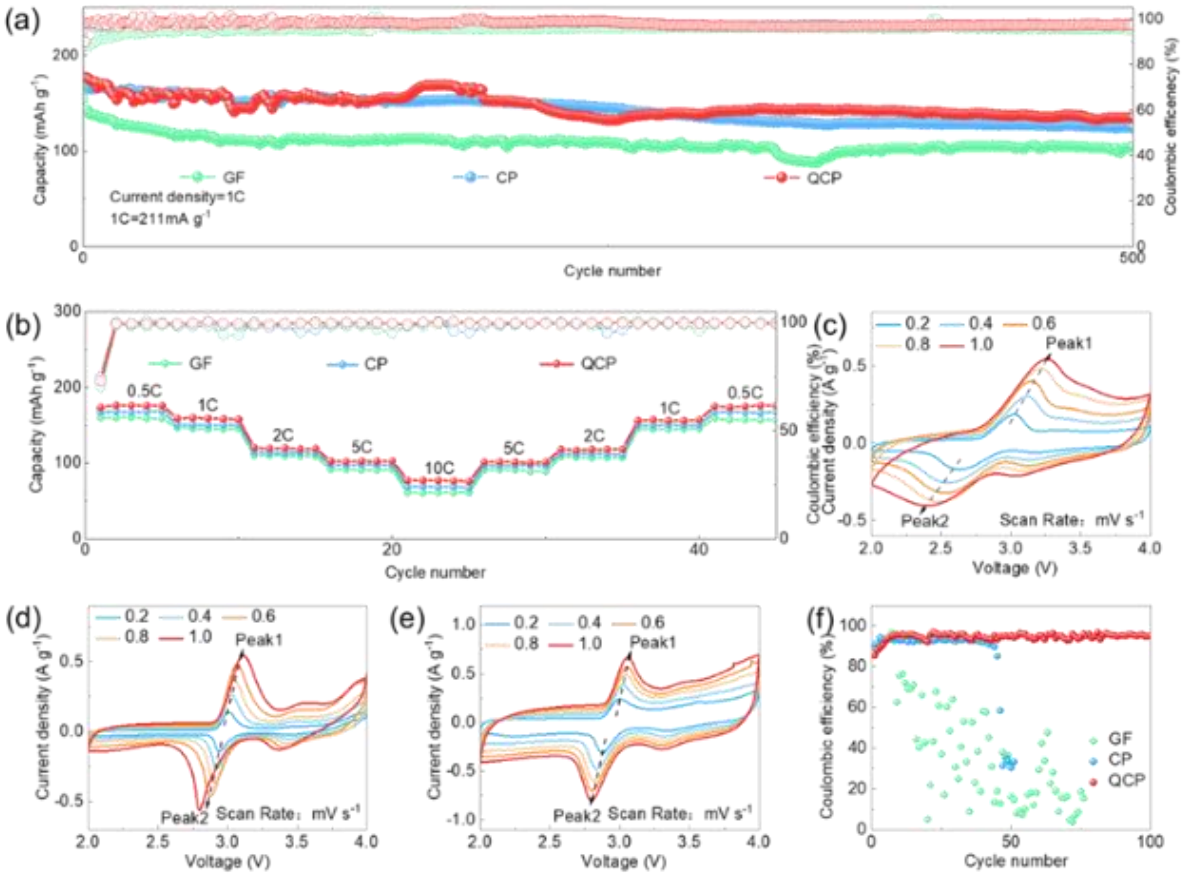

Figure 4. *(a) Cycling stability at 1 C; (b) Rate capability from 0.5 to 10 C; CV curves at scan rates from 0.2 to 1.0 mV s-1 of (c) GF, (d) CP, and (e) QCP; (f) Coulombic efficiency at 1 mA cm^{-2}, 1 mAh cm^{-2}.*

4. Conclusion

In conclusion, we have successfully developed a cationic quaternary ammonium cellulose separator (QCP) to regulate the transport and interfacial conversion behavior of iodide ions in lithium–iodine batteries. The introduction of quaternary ammonium groups creates a positively charged interface on the QCP separator, which selectively restricts negatively charged iodide species through electrostatic interactions. Compared with pristine glass fiber and cellulose separators, the QCP separator exhibits significantly enhanced iodide adsorption capacity, improved lithium-ion transference number, excellent ionic conductivity, and reduced interfacial resistance. Consequently, Li-I_2 batteries assembled with the QCP separator achieve substantial improvements in electrochemical reversibility, rate capability, and long-term cycling stability. Moreover, the QCP separator effectively stabilizes lithium deposition/stripping behavior and suppresses interfacial side reactions on the lithium metal anode. This work demonstrates that constructing a cationic cellulose interface is an effective strategy for selectively regulating polyiodide chemistry and enhancing the electrochemical performance of Li-I_2 batteries. More importantly, the proposed electrostatic ion-regulation mechanism offers new insights into separator–interface engineering for advanced halogen-based energy-storage systems.

Abbreviations

XRD	X-ray Diffraction
SEM	Scanning Electron Microscopy
EDS	Energy-dispersive X-ray Spectroscopy
CV	Cyclic Voltammetry

Author Contributions

Changyong Song: Conceptualization, Formal Analysis, Resources, Writing – original draft

Xuejin Li: Data curation, Funding acquisition, Methodology, Project administration

Wei Xing: Methodology, Supervision, Writing – review & editing

Funding

This work is supported by the Young Taishan Scholars Program of Shandong Province (tsqn202211082), the Natural Science Foundation of Shandong Province (ZR2023MB051, ZR2024QE082), National Natural Science Foundation of China (52277229, 52573362), the CNPC Innovation Foundation (2022DQ02–0410), the Taishan Industrial Experts Program, and the Fundamental Research Funds for the Central Universities (No. 26CX04033A).

Data Availability Statement

The data is available from the corresponding author upon reasonable request.

Conflicts of Interest

The authors declare no conflicts of interest.

References

[1] C. Li, J. Min, X. Zhang, S. Zhao, G. Qu, Q. Yu, M. Yang, D. Yuan, X. Xu, Efficient $I^-/I_3^-/I_2$ Conversion and Shuttle-Suppression in High-Rate Ah-Level Zinc-Iodine Batteries Enabled by Bifunctional Confined-Catalyst ZrB_2/AC Host, Angewandte Chemie International Edition 2026, e9794577. https://doi.org/10.1002/anie.9794577

[2] P. Li, X. Li, Y. Guo, C. Li, Y. Hou, H. Cui, R. Zhang, Z. Huang, Y. Zhao, Q. Li, B. Dong, C. Zhi, Highly Thermally/Electrochemically Stable I^-/I_3^- Bonded Organic Salts with High I Content for Long-Life Li–I_2 Batteries, Advanced Energy Materials 2022, 12(15). https://doi.org/10.1002/aenm.202103648

[3] D. Fan, J. Gong, S. Deng, H. Yan, Q. Zhu, H. Jiang, Progress and challenges of zinc-iodine flow batteries: From energy storage mechanism to key components, Journal of Energy Storage 2024, 92. https://doi.org/10.1016/j.est.2024.112215

[4] J. Lee, W. Lee, S. Back, S. Y. Yi, S. Lee, S. Kim, J. Moon, D.–Y. Koh, K. Kim, S. Back, J. Lee, Activating iodine redox by enabling single–atom coordination to dormant nitrogen sites to realize durable zinc–iodine batteries, EES Catalysis 2024, 2(1) 276–285. https://doi.org/10.1039/d3ey00228d

[5] C. Guan, Z. Lian, Z. Liu, E. I. Iwuoha, K. Ocakoglu, U. Feleni, L. Zhong, T. Li, X. Peng, Synergistic Physicochemical Confinement in a Dual–Functional Separator for Long–Life Zn–I_2 Batteries, ACS Applied Energy Materials 2026, 9(5) 2892–2901. https://doi.org/10.1021/acsaem.6c00169

[6] S. Chen, J. Ma, Q. Chen, W. Shang, J. Liu, J. Zhang, Exploring interfacial electrocatalysis for iodine redox conversion in zinc–iodine battery, Science Bulletin 2025, 70(4) 546–555. https://doi.org/10.1016/j.scib.2024.11.042

[7] W. Wu, C. Li, Z. Wang, H.–Y. Shi, Y. Song, X.–X. Liu, X. Sun, Electrode and electrolyte regulation to promote coulombic efficiency and cycling stability of aqueous zinc–iodine batteries, Chemical Engineering Journal 2022, 428. https://doi.org/10.1016/j.cej.2021.131283

[8] J. Ke, K. Bai, Z. Zhang, Z. Wen, J. Bu, Y. Tang, X. Liu, M. Ye, Y. Zhang, C. C. Li, Enabling I_3^-/I_2 Redox Couple toward High–Voltage Zn–Polyiodide Batteries by the Iodide–π Conjugation Effect, ACS Nano 2025, 19(18) 17746–17759. https://doi.org/10.1021/acsnano.5c02786

[9] J. Xu, W. Ma, L. Ge, M. Ren, X. Cai, W. Liu, J. Yao, C. Zhang, H. Zhao, Confining iodine into a biomass–derived hierarchically porous carbon as cathode material for high performance zinc–iodine battery, Journal of Alloys and Compounds 2022, 912. https://doi.org/10.1016/j.jallcom.2022.165151

[10] C. Song, Q. Wang, R. Wen, Q. Tang, Z. Luo, Z. Yuan, A Long-Life and Excellent Rate-Capability Aqueous Zn-Benzoquinone Battery Enabled by Iodine-Catalyzed Cathode, Small Methods 2023, 8(6). https://doi.org/10.1002/smtd.202300809

[11] W. Wang, R. Li, X. Xu, Y. Sun, Z. Sun, J. Yang, Y. Jiao, H. Wang, Electrocatalysts in zinc-iodine batteries: theoretical insights and material design, Coordination Chemistry Reviews 2025, 544. https://doi.org/10.1016/j.ccr.2025.216951

[12] W. Yuan, X. Qu, Y. Wang, X. Li, X. Ru, D. Jia, L. Zhao, Y. Hou, J. Shen, Z. Shen, N. Zhang, Polycationic polymer functionalized separator to stabilize aqueous zinc–iodine batteries, Energy Storage Materials 2025, 76. https://doi.org/10.1016/j.ensm.2025.104130

[13] L. Li, Y. C. A. Tsang, D. Xiao, G. Zhu, C. Zhi, Q. Chen, Phase–transition tailored nanoporous zinc metal electrodes for rechargeable alkaline zinc–nickel oxide hydroxide and zinc–air batteries, Nature Communications 2022, 13(1). https://doi.org/10.1038/s41467-022-30616-w

[14] J. Sun, H. Ma, D. Wang, Heavily heteroatoms doped carbons with tunable microstructure as the iodine hosts for rechargeable zinc–iodine aqueous batteries, Journal of Alloys and Compounds 2023, 947. https://doi.org/10.1016/j.jallcom.2023.169696

[15] J. Xu, Q. Dai, Y. Yang, Z. Zheng, F. Yu, Y. Cao, Z. Jiang, B. Peng, L. Ma, Wide–temperature zinc–iodine batteries enabling by a Zn–ion conducting covalent organic framework buffer layer, Chemical Engineering Journal 2024, 502. https://doi.org/10.1016/j.cej.2024.157984

[16] Z. Hu, X. Wang, W. Du, Z. Zhang, Y. Tang, M. Ye, Y. Zhang, X. Liu, Z. Wen, C. C. Li, Crowding Effect–Induced Zinc–Enriched/Water–Lean Polymer Interfacial Layer Toward Practical Zn–Iodine Batteries, ACS Nano 2023, 17(22). https://doi.org/10.1021/acsnano.3c10081

[17] J. Chen, C. Qiu, L. Zhang, B. Wang, P. Zhao, Y. Zhao, H. Wang, G. Yang, A. Sun, J. Fan, Q. Xv, O. J. Rojas, Wood–derived Fe cluster–reinforced asymmetric single–atom catalysts and weather–resistant organohydrogel for wide–temperature flexible Zn–air batteries, Energy & Environmental Science 2024, 17(13). https://doi.org/10.1039/d4ee01226g